

QUANTUM EFFICIENCY AND TRANSVERSE MOMENTUM FROM METALS *

T. Vecchione[#], D. Dowell, SLAC National Accelerator Laboratory, Menlo Park, CA 94025, U.S.A.
W. Wan, J. Feng, H. A. Padmore, LBNL, Berkeley, CA 94720, U.S.A.

Abstract

QE and transverse momentum are key parameters limiting the achievable brightness of FELs. Despite the importance, little data is available to substantiate current models. Expressions for each and experimental confirmation of each expression with respect to excess energy are presented. Novel instrumentation and analysis techniques developed are described.

INTRODUCTION

FELs are the next generation in high brightness accelerator based light sources. Because FEL brightness is ultimately limited by the quantum efficiency and transverse momentum of photocathodes confirmed expressions for each are important.

SINGLE CRYSTAL THEORY

The Sommerfeld model describes electronic states in metals. It has two components. The first is that electrons are bound by uniform potential and have kinetic energy measured with respect to it. The resulting density of states is constant. The second is that occupational probability is governed by Fermi-Dirac statistics with the chemical potential μ defined by the energy of the maximum occupied state at zero temperature. This gives an exponentially decaying occupational probability to states above the work function, ϕ .

The Spicer model identifies steps in photoemission. In the first step electrons absorb photons such that their momentum is increased normal to the surface only. Justification is given by observing that even in this case few states have sufficient momentum to escape. In the second step electrons diffuse to the surface where they escape in the third step based on their momentum. The surface barrier is treated as a well such that the bottom of the valence band is $\mu+\phi$ below the vacuum level. Photoexcited electrons traversing the barrier lose energy equal to $\mu+\phi-\hbar\omega$ in the direction normal to the surface. The probabilities associated with steps one and two are assumed to be represented by a constant S_{12} such that $0 \leq S_{12} \leq 1$. The probability associated with step three is given by the charge emitted per unit time per unit area assuming all electrons are ideally photoexcited divided by the current density normally incident on the surface.

Quantum Efficiency

QE is the number of emitted electrons per incident photon. The combination of Sommerfeld and Spicer

models produces an expression for QE, Eqn. 1. A consequence of the Fermi-Dirac distribution is that there is photoemission even when $\hbar\omega < \phi$. When $\hbar\omega - \phi \gg kT$ Eqn. 1. reduces to the Fowler-Dubridge equation.

$$QE = S_{12} \frac{\left(Li_2 \left[-Exp \left[\frac{e}{kT} (\hbar\omega - \phi) \right] \right] \right)}{\left(Li_2 \left[-Exp \left[\frac{e}{kT} \mu \right] \right] \right)} \quad (1)$$

The differential of the emitted current density, dJ/dr , expressed in external cylindrical coordinates and normalized to unity at $p_r=0$ gives the transverse momentum distribution, Eqn. 2.

$$\frac{dJ_r}{dJ_0} = \frac{Li_1 \left[-Exp \left[\frac{e}{kT} (\hbar\omega - \phi) - \frac{1}{2mkT} \left(\frac{mc}{1000} \right)^2 p_r^2 \right] \right]}{Li_1 \left[-Exp \left[\frac{e}{kT} (\hbar\omega - \phi) \right] \right]} \quad (2)$$

The polylogarithm functions used here are defined by Eqn. 3.

$$Li_n[z] = \frac{(-1)^{n-1}}{(n-2)!} \int_0^1 \frac{1}{t} Log[t]^{n-2} Log[1-zt] dt \quad (3)$$

RMS Transverse Momentum

The combination of Sommerfeld and Spicer models produces an expression for RMS transverse momentum ϵ_x , Eqn. 4, including a $\sqrt{2}$ to convert to Cartesian coordinates.

$$\epsilon_x = 1000 \sqrt{\frac{kT}{mc^2}} \sqrt{\frac{Li_3 \left[-Exp \left[\frac{e}{kT} (\hbar\omega - \phi) \right] \right]}{Li_2 \left[-Exp \left[\frac{e}{kT} (\hbar\omega - \phi) \right] \right]}} \quad (4)$$

The RMS transverse momentum is non-zero even when $\hbar\omega < \phi$. In the limit of $\hbar\omega=0$ and $\phi < kT$, Eqn. 4 equals the RMS transverse momentum of thermal emission. In the limit of $\hbar\omega - \phi \gg kT$ Eqn. 4 reduces to the Dowell equation.

METHODS

Sample Preparation

10 nm thin films of aluminum were deposited onto doped silicon. The substrates were first dipped in hydrofluoric acid and then flashed in vacuum. Next films were deposited at room temperature using a DC sputter gun. A quartz crystal monitor measured the rates. Chamber pressures were $1-2 \times 10^{-10}$ torr. Finally H_2O and O_2 were used to oxidize the films.

*Work supported by US DOE contracts DE-AC02-05CH11231, KC0407-ALSJNT-10013, and DE-SC000571.

[#]tvecchio@slac.stanford.edu

Illumination

A light source was developed to provide instrumental resolution less than kT. The high brightness fiber coupled system was based on a laser plasma source. The monochromator used matched 100 μm slits and a 1200 g/mm grating. Flux calibrations were performed using a photodiode and an electrometer. Typical performance in the UV was 1x10¹² ph/sec at 1-2 nm FWHM bandpass.

Quantum Efficiency Measurement

Light was collimated and incident through a fused quartz viewport. Biased -10 V currents were recorded using an electrometer with system noise levels on the order of tens of femtoamperes.

Transverse Momentum Measurement

Electrons were accelerated by a field of up to 3 MV/m generated by an applied voltage V between a photocathode and a mesh grid anode. The two were separated by a gap, g = 5 mm. The grid had a 25.4 μm mesh and formed an immersion lens with a field free region allowing the beam to expand by drifting a distance, d = 244 mm. A camera imaged a phosphor screen behind a channel plate. Light was focused through the grid at 30° wrt the surface into a 150 μm spot.

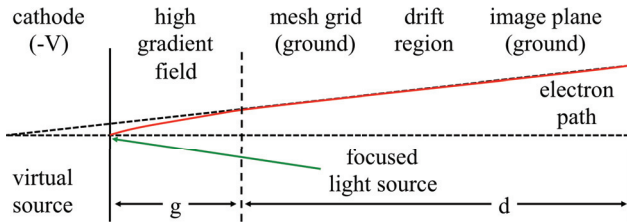


Figure 1: Arrangement for measuring transverse momentum.

The transverse momentum, p_r, of an electron at the image plane is related to its radial coordinate, r, by Eqn. 5.

$$p_r = 1000 \sqrt{\frac{2eV}{mc^2}} \left(\frac{r}{2g+d} \right) \tag{5}$$

SINGLE CRYSTAL ANALYSIS

Transverse Momentum Distributions

Transverse momentum distributions are shown in Fig. 2. The fits match well over the first 0.5 eV of excess energy. Some electrons are observed to have larger than expected transverse momentum. This may come from either instrumental resolution or spacecharge effects.

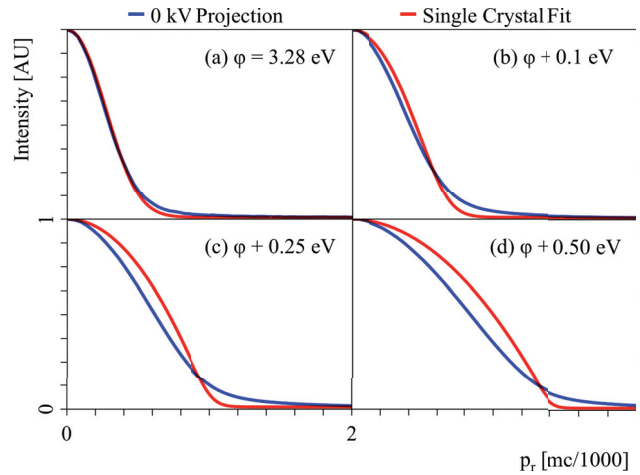


Figure 2: Transverse momentum distributions and single crystal fits from oxidized aluminum at several values of excess energy.

RMS Transverse Momentum

RMS transverse momentum is shown in Fig 3. Two observations are made. First, RMS transverse momentum plateaus at ~0.225 μm/mm as predicted by Eqn. 4. Second, model RMS transverse momentum is less than measured due to electrons with larger than expected transverse momentum as discussed above.

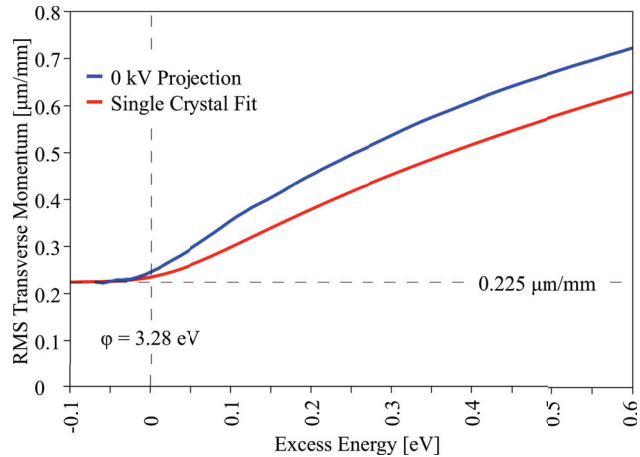


Figure 3: RMS transverse momentum from oxidized aluminum.

POLYCRYSTALLINE EXTENSION

Thin films can be polycrystalline. In this case the distribution of work functions should be measured and summed accordingly. The polycrystalline approximation attempts to simulate this by assuming a range of work functions Δφ extending from φ to φ+Δφ with equal representation for each.

Quantum Efficiency

The polycrystalline analog of Eqn. 1 is Eqn. 6.

QE is shown in Fig. 4. Several observations are made. First, QE gradually increases at the onset. Second, the work function obtained matches published values. Third, at 0.5 eV excess energy the value of QE is 1×10^{-4} . Fourth, the work function drops by ~ 1 eV during oxidization. Finally, the data fit well to the polycrystalline model.

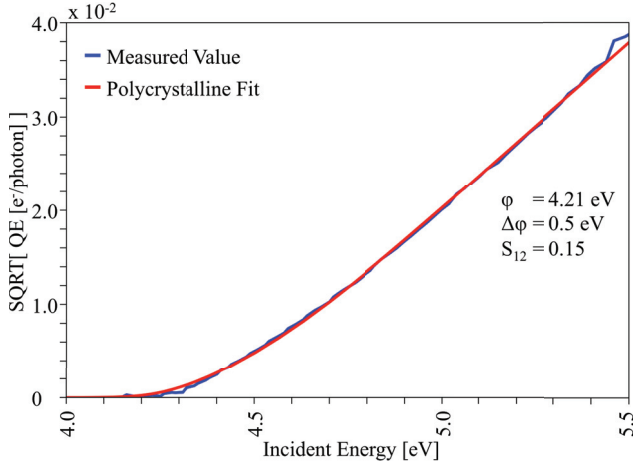


Figure 4: Fowler plot for aluminum prior to oxidization.

Transverse Momentum Distributions

The polycrystalline analog of Eqn. 2 is Eqn. 7.

Transverse momentum distributions are shown in Fig 5. The data fit better to the polycrystalline model than they do to the single crystal model.

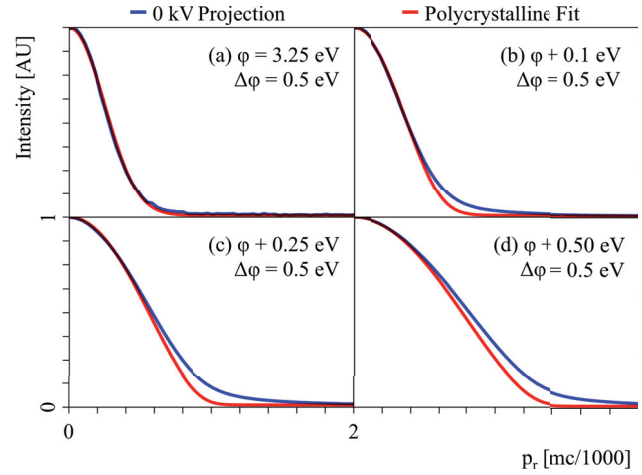


Figure 5: Transverse momentum distributions and polycrystalline fits from oxidized aluminum at several values of excess energy.

The polycrystalline analog of Eqn. 4 is Eqn. 8.

CONCLUSIONS

QE and transverse momentum are key parameters limiting the achievable brightness of free-electron lasers. Expressions for each and experimental confirmation of each expression with respect to excess energy were presented. Observations that QE undergoes a gradual onset at the work function and that transverse momentum plateaus at its thermal limit are both attributed to the Fermi-Dirac distribution.

$$QE = S_{12} \left(\frac{kT}{e\Delta\phi} \right) \left(\frac{Li_3 \left[-Exp \left[\frac{e}{kT} (\hbar\omega - \phi) \right] \right] - Li_3 \left[-Exp \left[\frac{e}{kT} (\hbar\omega - \phi - \Delta\phi) \right] \right]}{Li_2 \left[-Exp \left[\frac{e}{kT} \mu \right] \right]} \right) \quad (6)$$

$$\frac{dJ_r}{dJ_0} = \frac{Li_2 \left[-Exp \left[\frac{e}{kT} (\hbar\omega - \phi) - \frac{1}{2mkT} \left(\frac{mc}{1000} \right)^2 p_r^2 \right] \right] - Li_2 \left[-Exp \left[\frac{e}{kT} (\hbar\omega - \phi - \Delta\phi) - \frac{1}{2mkT} \left(\frac{mc}{1000} \right)^2 p_r^2 \right] \right]}{Li_2 \left[-Exp \left[\frac{e}{kT} (\hbar\omega - \phi) \right] \right] - Li_2 \left[-Exp \left[\frac{e}{kT} (\hbar\omega - \phi - \Delta\phi) \right] \right]} \quad (7)$$

$$\varepsilon_x = 1000 \sqrt{\frac{kT}{mc^2}} \sqrt{\frac{Li_4 \left[-Exp \left[\frac{e}{kT} (\hbar\omega - \phi) \right] \right] - Li_4 \left[-Exp \left[\frac{e}{kT} (\hbar\omega - \phi - \Delta\phi) \right] \right]}{Li_3 \left[-Exp \left[\frac{e}{kT} (\hbar\omega - \phi) \right] \right] - Li_3 \left[-Exp \left[\frac{e}{kT} (\hbar\omega - \phi - \Delta\phi) \right] \right]}} \quad (8)$$